PNAS
www.pnas.org

Supplementary Information for

Acoustofluidic Sonoporation for Gene Delivery to Human Hematopoietic Stem and Progenitor Cells

J. N. Belling, L. K. Heidenreich, Z. Tian, A. M. Mendoza, T. Chiou, Y. Gong, N. Y. Chen, T. D. Young, N. Wattanatorn, J. H. Park, L. Scarabelli, N. Chiang, J. Takahashi, S. Young, A. Steig, S. De Olveira, T. J. Huang, P. S. Weiss, and S. J. Jonas

Paul S. Weiss
Email: psw@cnsi.ucla.edu

Steven J. Jonas
Email: sjjonas@mednet.ucla.edu

This PDF file includes:

Supplementary Information Materials and Methods
Figs. S1 to S7
Caption for movies S1

Other supplementary materials for this manuscript include the following:

Movie S1

www.pnas.org/cgi/doi/10.1073/pnas.1917125117

SI Materials and Methods

Simulation. Commercial finite element analysis software, COMSOL Multiphysics, was used for simulating the pressure field in the glass capillary. A solid mechanics module was used to model the glass capillary with a density, Young's modulus, and Poisson's ratio set at 2,200 kg/m^3, 72 GPa, and 0.17 respectively. A pressure acoustic module was used to model the liquid medium by setting density and speed of sound at 1,000 kg/m^3 and 1,480 m/s respectively. Continuity boundary conditions are applied to the left and right boundaries of the model and a harmonic force is applied to the top boundary of the glass capillary to simulate the excitation force from the lead zirconate titanate (PZT) transducer.

Statistical and Image Analyses. One-way ANOVA analyses were performed using Origin 9.1 data analysis and graphing software. Quantification of DAPI-GFP co-localization, and DNA damage utilized Fiji image analysis software and the cell counter plugin.

Materials and Data Availability. All original data are available in the manuscript and supplementary information. Materials are available either commercially or upon request.

Supplementary Figures

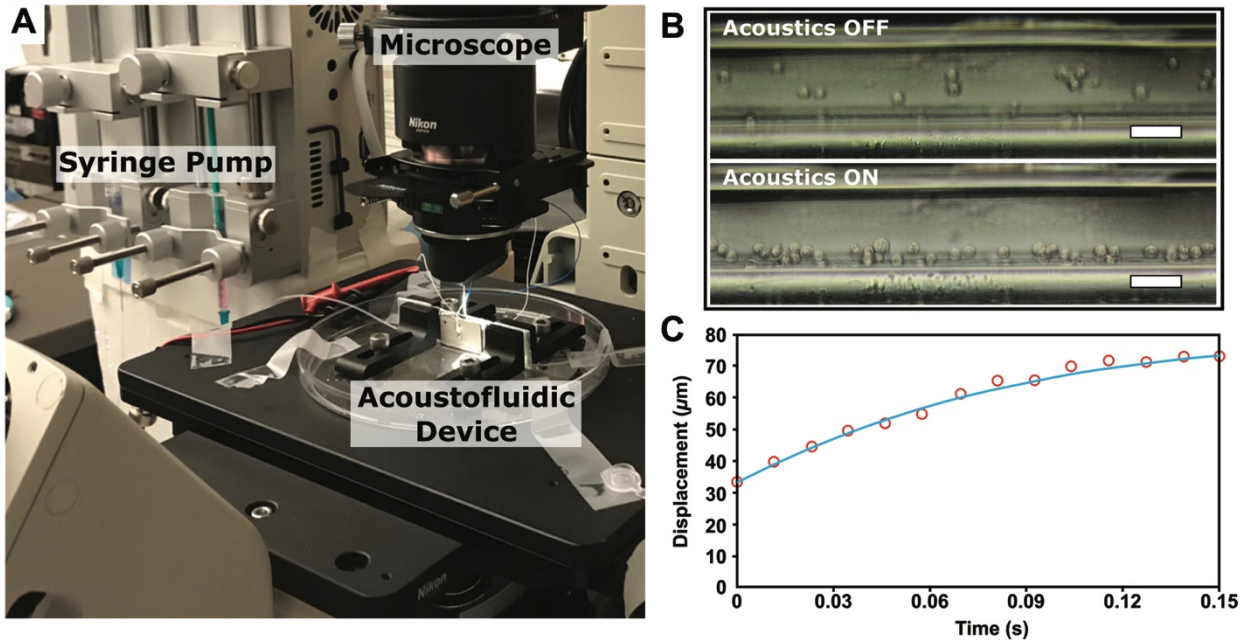

Fig. S1. (A) Custom stage setup to image the cross section of the glass capillary, where the acoustofluidic device is fixed vertically between two sliders that are attached to a Petri dish and placed above a microscope objective. **(B)** Images of Jurkat cells with (Acoustics ON) and without (Acoustics OFF) an applied electrical potential without flow. **(C)** Jurkat cell displacement from the transducer as a function of time. The red circles represent experimental data extracted from the recorded video of cell movement at the acoustic excitation frequency of 3.3 MHz with an amplitude of 40 V peak-to-peak. The solid line is obtained by fitting the experimental data to a theoretical cell displacement relation for resonator-based acoustic tweezers (39). From the fit curve, we can identify the acoustic energy density, and estimate the pressure amplitude and acoustic radiation force exerted on the cell. Scale bars are 50 μm.

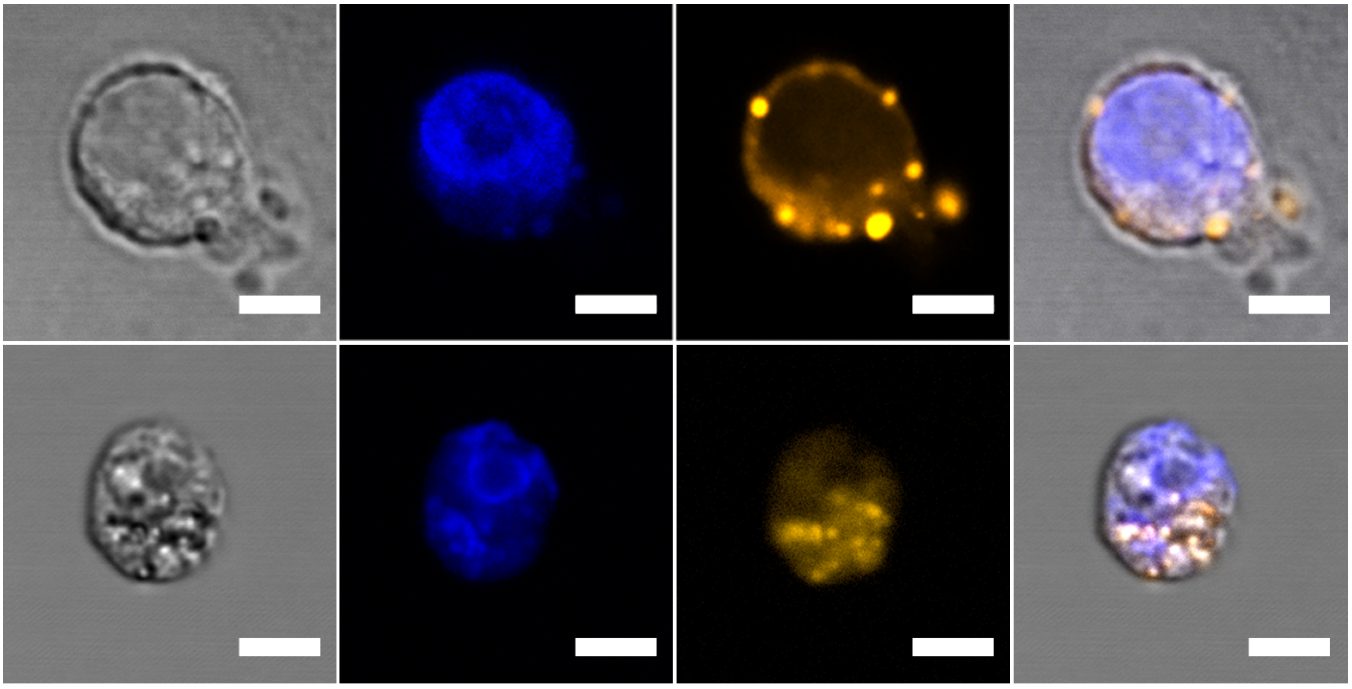

Fig. S2. Brightfield images and confocal laser scanning micrographs of Jurkat cells post-acoustofluidic delivery of Alexafluor 546-labeled DNA (Cy3-DNA). The Cy3-DNA (orange) is shown distributed throughout the cell cytosol, on the cell membrane, and at the cell nucleus that has been stained with DAPI (blue). Scale bars are 10 μm.

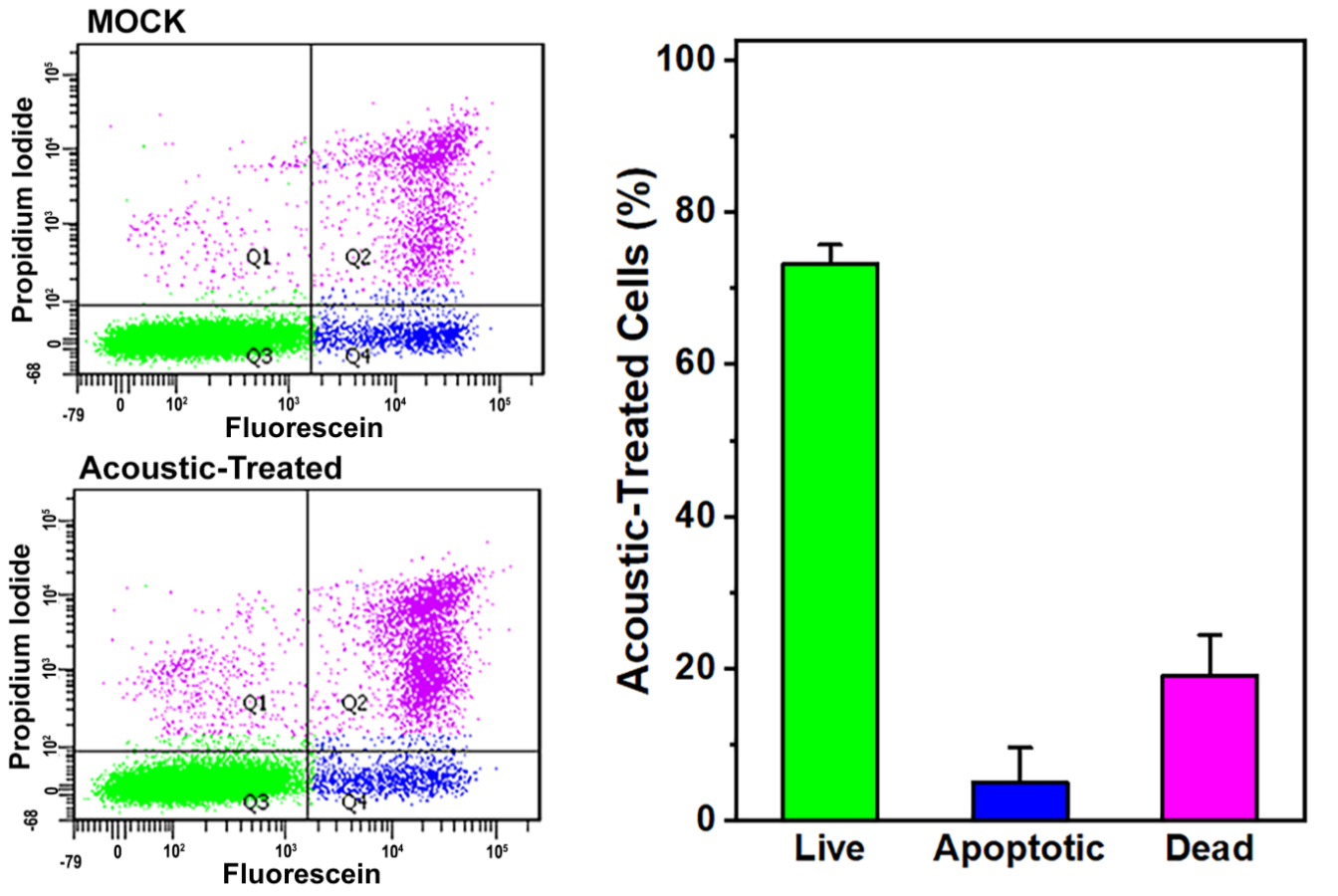

Fig S3. Flow cytometric analysis of cell viability using an Annexin V-propidium iodide assay with untreated (mock) and post-acoustofluidic-treated Jurkat cells. Representative density plots with gating for mock and acoustic samples are shown on the left and the data are expressed as the mean and standard deviation for N=5.

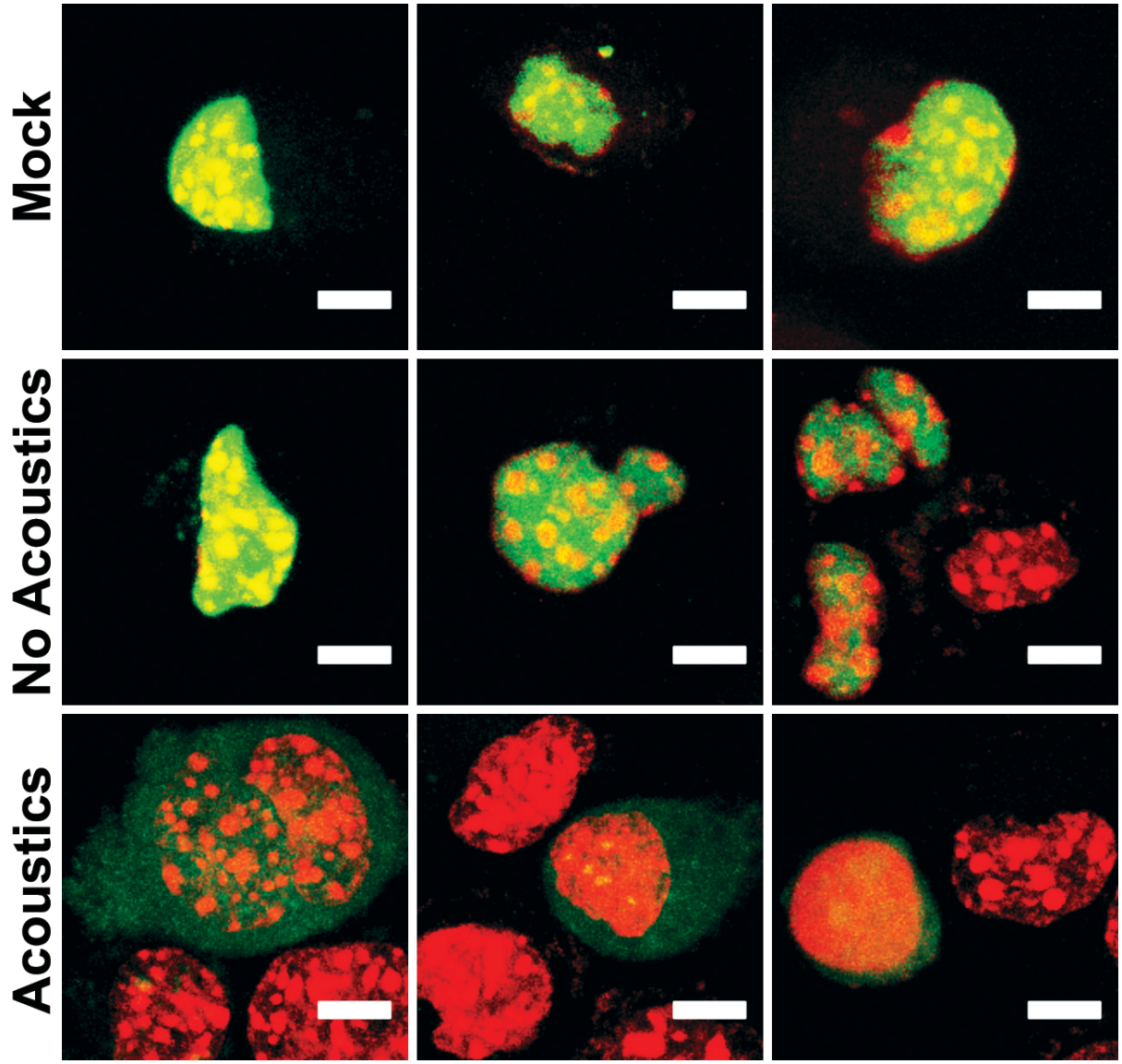

Fig. S4. Confocal laser scanning micrographs of MEFs at 100× magnification, showing colocalization events of green fluorescent protein fused to a nuclear localization signal (NLS-GFP) and DAPI signals in the untreated (Mock), no acoustics (No Acoustics), and acoustic-treated (Acosutics) samples. The MEFs are virally transduced to express GFP at their nuclei (green) and are stained post-acoustofluidic treatment with DAPI to label the cell nuclei (red). Co-localization of NLS-GFP and DAPI signals are shown in the overlay of the mock and no-acoustics samples and lack thereof (as shown in the acoustic-treated samples) is evidence of nuclear membrane rupture. Scale bars are 10 μm.

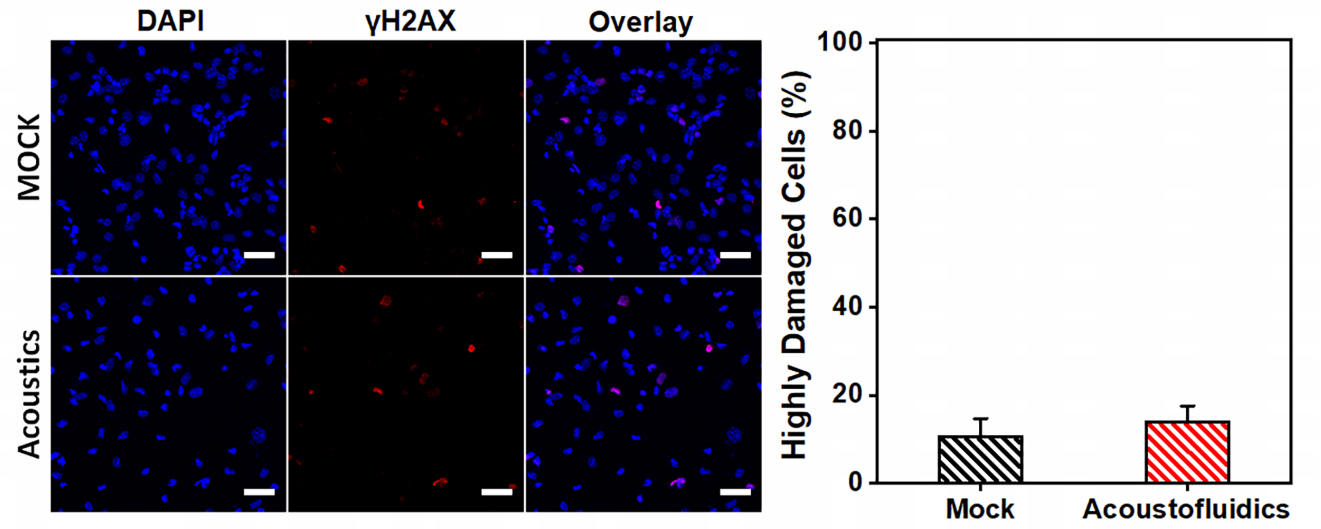

Fig. S5. Immunofluorescence microscopy of untreated (mock), and acoustofluidic-treated mouse embryonic fibroblasts that had been fixed and then stained with an antibody against the DNA damage marker γH2AX (red) and nuclear stain DAPI (blue). Highly damaged cells are identified as having >7 labeled DNA foci and data are expressed as mean and standard deviation for N=3. Scale bars are 50 μm.

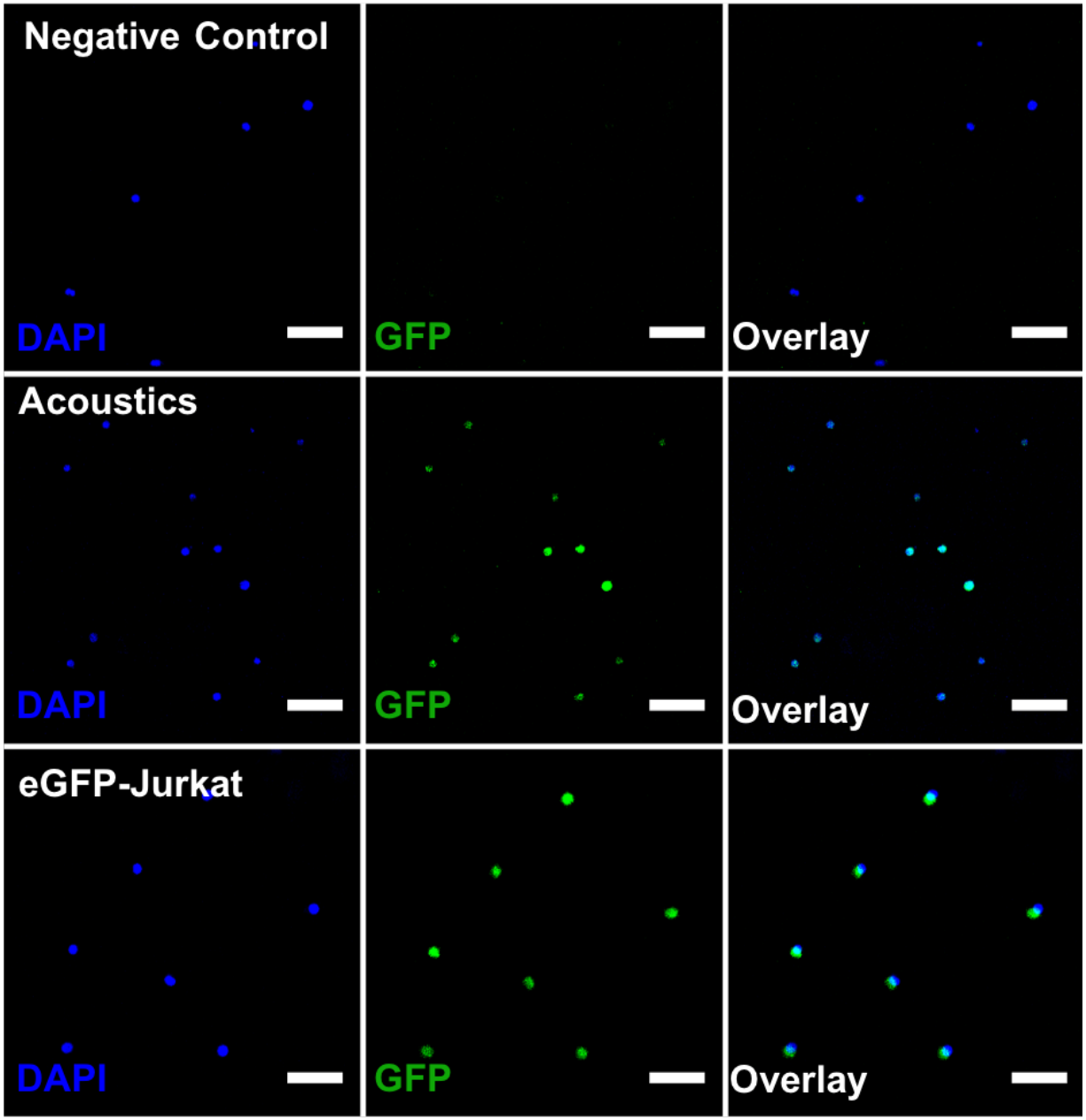

Fig. S6. Confocal laser scanning micrographs of untreated mixed donor umbilical cord blood $CD34^+$ hematopoietic stem and progenitor (CD34+) cells (Negative Control), 72 h post-acoustofluidic delivery of an enhanced green fluorescent protein-expressing plasmid (GFP) to CD34+ cells (Acoustics), and an eGFP-expressing Jurkat cell line (eGFP-Jurkat) as a positive control. A nuclear stain (DAPI) was used to determine cell location. Scale bars are 50 μm.

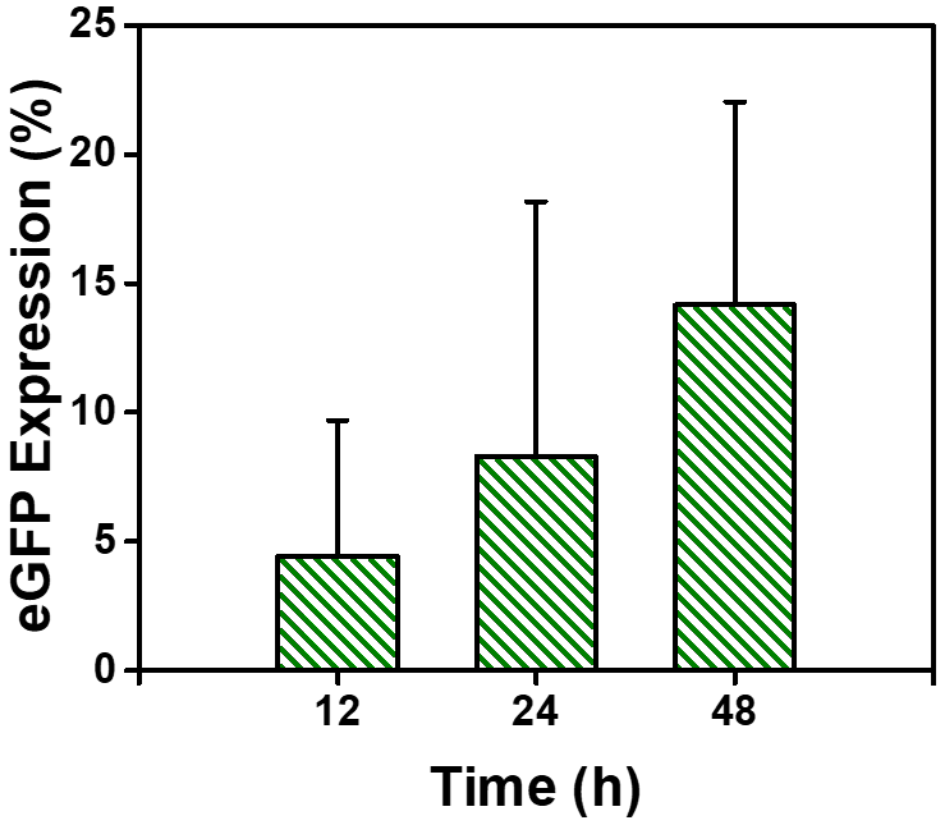

Fig. S7. Time response of enhanced green fluorescent protein (eGFP) expression measured over a 48 h period post-acoustofluidic delivery of an eGFP-expression plasmid to peripheral blood mononuclear cells. Data are expressed as mean and standard deviation for N=3.

Caption for Movie S1

Movie S1. High-speed imaging of acoustofluidic treatment. Sequential images of Jurkat cells introduced into the glass capillary at a flow rate of 192 μL/min. A constant input peak-to-peak voltage of 40 V was applied to the piezoelectric transducer while cells were flowed into the glass capillary.